Microwave photonic notch filter with complex coefficient based on four wave mixing*

XU Dong (许东)[1], **CAO Ye** (曹晔)[2]**, **TONG Zheng-rong** (童峥嵘)[1], **and YANG Jing-peng** (杨菁芃)[1]

1. Communication Devices and Technology Engineering Research Center, School of Computer and Communication Engineering, Tianjin University of Technology, Tianjin 300384, China

2. School of Electronic and Information Engineering, Qingdao University, Qingdao 266071, China

(Received 21 July 2016)

A microwave photonic notch filter with a complex coefficient is proposed and demonstrated based on four wave mixing (FWM). FWM effect of two single-frequency laser beams occurs in a highly nonlinear fiber (HNLF), and multi-wavelength optical signals are generated and used to generate the multi-tap of microwave photonic filter (MPF). The complex coefficient is generated by using a Fourier-domain optical processor (FD-OP) to control the amplitude and phase of the optical carrier and phase modulation sidebands. The results show that this filter can be changed from bandpass filter to notch filter by controlling the FD-OP. The center frequency of the notch filter can be continuously tuned from 5.853 GHz to 29.311 GHz with free spectral range (*FSR*) of 11.729 GHz. The shape of the frequency response keeps unchanged when the phase is tuned.

Document code: A **Article ID:** 1673-1905(2016)06-0417-4

DOI 10.1007/s11801-016-6167-2

Microwave photonic filter (MPF) has attracted considerable attention in the past years due to its immunity to electromagnetic interference[1-4], wide range of potential applications and advantages in terms of bandwidth, tunability[5-7] and reconfigurability[8,9] compared with traditional radio-frequency (RF) circuits.

In general, MPF with positive coefficients can only be used as low-pass filters, and MPF with negative coefficients can be used as bandpass filters, while the notch filter with complex coefficients is required in many systems to remove the interference signals. Up to now, many microwave photonic notch filters with different coefficients have been reported[10-16] including those based on dual-parallel Mach-Zehnder modulator (DP-MZM)[10], single-sideband (SSB) modulation[11], stimulated Brillouin scattering[12,13], optical bandpass filter (OBPF)[14] and fiber Bragg grating (FBG)[15]. However, the SSB modulator and DP-MZM modulator have the problem of bias drift, and the 90° hybrid coupler limits the bandwidth of the notch filter. The SBS-based MPF has a complicated and bulky structure because two or more electro-optic modulators are needed. The notch filter using a polarization modulator, an OBPF, an optical time delay line (OTDL) and a variable optical attenuator (VOA) may bring certain advantages but complexity. The free spectral range (*FSR*) of the proposed filter is small. The single-notch MPF using FBG suffers from the frequency drift between the tunable laser diode and the FBG resonance. Note that most schemes are achieved by one tap or two taps which may bring certain disadvantages, including low-resolution of notch filter and high cost.

In this paper, we demonstrate a novel and simple microwave photonic notch filter with complex coefficient based on four wave mixing (FWM). The FWM effect of two single-frequency laser beams occurs in a highly nonlinear fiber (HNLF), and multi-wavelength optical signal output is generated, which is used to generate the multi-tap of the MPF. The complex coefficient is generated using a diffraction-based Fourier-domain optical processor (FD-OP) to control the amplitude and phase of the optical carrier and RF phase modulation sidebands. Therefore, the filter can be switched from bandpass filter to notch filter and tuned over the entire *FSR*, while the shape of the frequency response remains unaltered.

The schematic diagram of the proposed microwave photonic notch filter is shown in Fig.1, which mainly consists of a multi-wavelength light source, a phase modulator (PM), an FD-OP, a dispersive medium and a photodetector (PD).

* This work has been supported by the National High Technology Research and Development Program of China (863 Program) (No.2013AA014200), the National Natural Science Foundation of China (No.11444001), and the Municipal Natural Science Foundation of Tianjin (No.14JCYBJC16500).

** E-mail: cynever@163.com

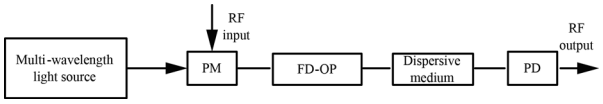

Fig.1 Schematic diagram of the proposed microwave photonic filter

In the proposed system, the output multi-wavelength optical signal is modulated using a PM by the microwave signal. The optical field at the output of PM can be written as

$$E_{\mathrm{PM}}(t)=\sum_{m=1}^{M}E_{\mathrm{c},m}\exp\mathrm{j}[\omega_{\mathrm{c},m}t+k_{\mathrm{p}}\cos(\omega_{\mathrm{RF}}t)]\,, \tag{1}$$

where m is the wavelength index, $E_{\mathrm{c},m}$ and $\omega_{\mathrm{c},m}$ are the amplitude of the electric field and the angular frequency of the mth input optical carrier, respectively, and ω_{RF} is the applied electrical drive signal. $k_{\mathrm{p}}=\pi V_{\mathrm{RF}}/V_{\pi}$ is the modulation index, where V_{π} is the half-wave voltage of the PM, and V_{RF} is the amplitude of the microwave signal. Based on the Jacobi-Anger expansions, considering small-signal modulation, Eq.(1) can be expanded as

$$E_{\mathrm{PM}}(t)=\sum_{m=1}^{M}E_{\mathrm{c},m}[J_0(k_{\mathrm{p}})\exp\mathrm{j}(\omega_{\mathrm{c},m}t)+$$

$$J_1(k_{\mathrm{p}})\exp\mathrm{j}(\omega_{\mathrm{c},m}+\omega_{\mathrm{RF}})t-J_1(k_{\mathrm{p}})\exp\mathrm{j}(\omega_{\mathrm{c},m}-\omega_{\mathrm{RF}})t]\,, \tag{2}$$

where $J_n(k_{\mathrm{p}})$ is the nth order Bessel function of the first kind. Note that the phases of the two sidebands are opposite. When phase modulation signal is directly sent to PD, there is no RF signal at the PD output, because the beating between the anti-phase sidebands and the carrier exactly offsets. And then the modulated light is launched into FD-OP. The FD-OP works as a programmable optical filter. This signal passes through an FD-OP which is programmed to remove the lower sideband of the RF phase modulated optical signal, to introduce a phase shift to the carrier and upper sideband and to control the amplitude of carrier and the upper sideband, as shown in Fig.2. The resulting output optical filed becomes

$$E_{\mathrm{PD\text{-}OP}}(t)=\sum_{m=1}^{M}E_{\mathrm{c},m}\left\{\sqrt{a_{\mathrm{c},m}}J_0(k_{\mathrm{p}})\exp\mathrm{j}(\omega_{\mathrm{c},m}t+\varphi_{\mathrm{c},m})+\right.$$

$$\left.\sqrt{a_{\mathrm{s},m}}J_1(k_{\mathrm{p}})\exp\mathrm{j}[(\omega_{\mathrm{c},m}+\omega_{\mathrm{RF}})t+\varphi_{\mathrm{s},m}]\right\}, \tag{3}$$

where $\sqrt{a_{\mathrm{c},m}}$ and $\sqrt{a_{\mathrm{s},m}}$ are the power attenuations of the mth optical carrier and upper sideband, respectively, and $\varphi_{\mathrm{c},m}$ and $\varphi_{\mathrm{s},m}$ are the phase shifts of the mth optical carrier and upper sideband, respectively. The dispersive medium introduces time delay to different optical carriers and upper sidebands. The optical filed behind the dispersive medium can be expressed as

$$E_{\mathrm{out}}(t)=\sum_{m=1}^{M}E_{\mathrm{c},m}\left\{\sqrt{a_{\mathrm{c},m}}J_0(k_{\mathrm{p}})\times\right.$$

$$\exp\mathrm{j}[\omega_{\mathrm{c},m}(t+(m-1)\tau)+\varphi_{\mathrm{c},m}]+\sqrt{a_{\mathrm{s},m}}J_1(k_{\mathrm{p}})\times$$

$$\left.\exp\mathrm{j}[(\omega_{\mathrm{c},m}+\omega_{\mathrm{RF}})(t+(m-1)\tau)+\varphi_{\mathrm{s},m}]\right\}, \tag{4}$$

where $\tau=\Delta\lambda DL$ is the basic time delay, $\Delta\lambda$ is the wavelength separation, D is the dispersion parameter of the dispersive medium with a unit of ps/nm, and L is the length of the dispersive medium.

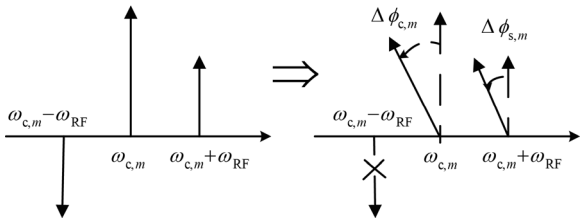

Fig.2 Schematic diagram of optical spectra at different locations

The optical power at the RF into the PD, which is the optical filed square, is given by[16]

$$P_{\mathrm{out}}=2J_0(k_{\mathrm{p}})J_1(k_{\mathrm{p}})\sqrt{A^2+B^2}\,, \tag{5}$$

where

$$A=\sum_{m=1}^{M}P_{\mathrm{in},m}\sqrt{a_{\mathrm{c},m}}\sqrt{a_{\mathrm{s},m}}\cos[\omega_{\mathrm{RF}}(m-1)\tau+\Delta\varphi_m]\,, \tag{6}$$

$$B=\sum_{m=1}^{M}P_{\mathrm{in},m}\sqrt{a_{\mathrm{c},m}}\sqrt{a_{\mathrm{s},m}}\sin[\omega_{\mathrm{RF}}(m-1)\tau+\Delta\varphi_m]\,, \tag{7}$$

where $P_{\mathrm{in},m}$ is the optical power of the mth optical carrier, and $\Delta\varphi_m=\Delta\varphi_{\mathrm{s},m}-\Delta\varphi_{\mathrm{c},m}$. Under the small signal condition, the filter transfer function, which is defined as the ratio of the output RF signal power to input RF signal power, can be obtained and written as

$$\left|H(f_{\mathrm{RF}})\right|^2=\left(\frac{\pi}{V_{\pi}}\right)^2R_{\mathrm{in}}R_{\mathrm{o}}\Re^2(A^2+B^2)\,, \tag{8}$$

where $\Re$ is the photodiode response, R_{in} is the modulator input resistance, and R_{o} is the PD load resistance.

Thanks to the optical phase control function in the FD-OP, the notch frequency can be continuously tuned by designing the phase shift of the mth tap to be

$$\Delta\varphi_{m\mathrm{th}}=\Delta\varphi'_m+m\theta\,, \tag{9}$$

where $\Delta\varphi'_m$ is the original phase shift of the mth tap and is either 0° or 180°, and $m\theta$ is the extra phase required to be added to the mth tap for tuning the notch frequency. The notch frequency is given by

$$f_{\mathrm{notch}}=f'_{\mathrm{nocth}}+\frac{\theta}{2\pi\tau}\,, \tag{10}$$

where f'_{notch} is the original notch frequency.

The configuration of the proposed MPF is shown in Fig.3, and the schematic diagram of the multi-wavelength light source is in the dashed box. The multi-wavelength light source is generated by a broaden spec-

trum, which is caused by FWM effect. The single-frequency laser beams from tunable laser 1 and tunable laser 2 are emitted into an HNLF, and an erbium-doped fiber amplifier (EDFA) is used to amplify the laser power, in order to excite FWM effect in the HNLF, which can broaden the spectrum of the input optical signal. The output spectrum with four output wavelengths is shown in Fig.4. The wavelengths of the tunable laser 1 and the tunable laser 2 are 1 549.85 nm and 1 550.85 nm, respectively, i.e., the wavelength difference of the two lasers is 1 nm. A polarization controller (PC) is used to align the optical signal polarization state to maximize the efficiency of the PM. The frequency range of the analog signal generator is from 1 GHz to 43 GHz. The modulation frequency of the PM is 40 GHz. The phase modulated optical signal is amplified by an EDFA, and is processed by an FD-OP (Finisar waveshaper 4000S with the resolution of 1 GHz), which is measured with help of the amplified optical signal from an EDFA. The waveshaper introduces an optical power attenuation of 6 dB to the upper sideband and the optical carrier, respectively. A 5-km-long single-mode fiber (SMF) is used as the dispersion device, the dispersion at 1 550 nm is 17.9 ps/(nm·km), and the total accumulated dispersion is 89.5 ps/nm. After being processed in the dispersion medium, the light is launched into a PD with a bandwidth of 40 GHz. We use a 40 GHz spectrum analyzer to measure the phase shift of the recovered RF signal.

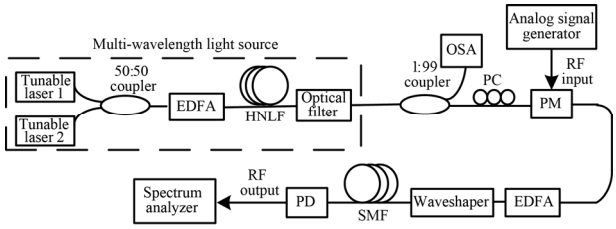

Fig.3 Schematic diagram of the filter and the multi-wavelength light source

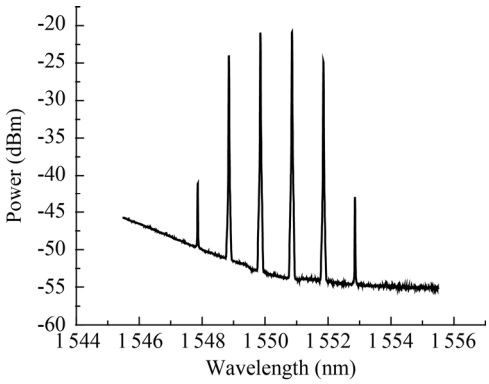

Fig.4 Output spectrum of the multi-wavelength light source with Δλ=1 nm

This filter can transform from bandpass to notch filter by controlling the FD-OP. Fig.5 shows the simulated and measured frequency responses of the 4-tap bandpass MPF. The MPF has an *FSR* of 11.729 GHz. The FD-OP does nothing. The four taps have the same phase and lower sideband. Fig.6 shows the measured and simulated frequency responses of the 4-tap bandstop MPF. By programming the FD-OP, the middle two taps have the same amplitude and the same phase of 0°. The next pair of taps has a 180° phase difference relative to the middle two taps. The frequencies of the notch 1 and notch 2 are 17.582 GHz and 29.311 GHz, respectively, i.e., the *FSR* of this MPF is 11.729 GHz. As shown in Figs.5 and 6, the simulated results match the measured results very well.

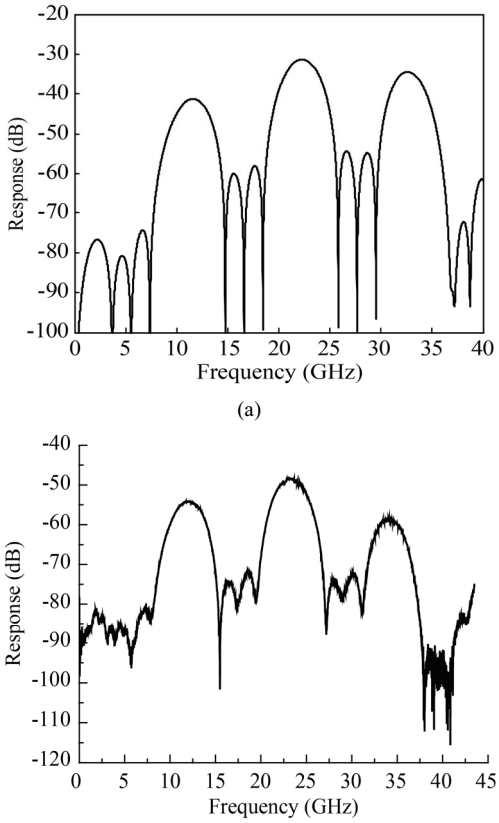

Fig.5 (a) Simulated and (b) measured frequency responses of the 4-tap bandpass MPF

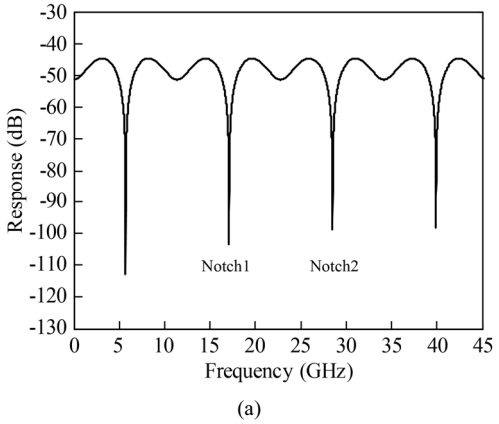

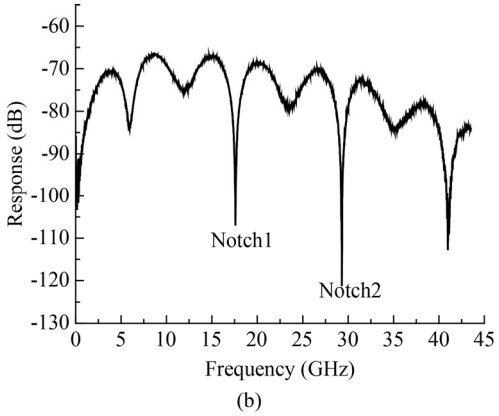

Fig.6 (a) Simulated and (b) measured frequency responses of the 4-tap bandstop MPF

Fig.7 shows the frequency responses of the notch MPF with different phases. The notch position of the MPF is continuously tuned in the entire *FSR* when the shifter of the optical carrier is changed in 2π. When the phase shift coefficient is positive, the notch 1 moves to the right. And when the phase shift coefficient is negative, the notch 1 moves to the left. It must be pointed that by adjusting phase θ, the notch frequency is tuned from 5.853 GHz to 29.311 GHz. The notch position of the filter is varied, while the shape and the *FSR* of the frequency response both remain unchanged.

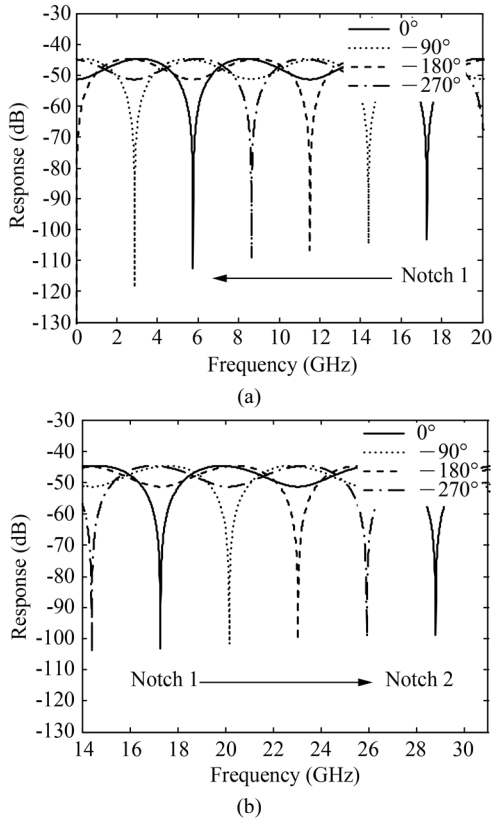

Fig.7 The frequency responses of the notch MPF with different phases for (a) negative and (b) positive phase shift coefficients

It must be pointed that the *FSR* of the filter is unchanged, and the filter response has a low resolution. The *FSR* of the filter can be tuned by changing the frequency difference of two input laser beams. The multi-wavelength laser outputs four wavelengths in this experiment. If longer HNLF and more powerful EDFA are engaged, the multi-wavelength laser will output more wavelengths. Then the notch filter resolution can be enhanced.

We propose and demonstrate a microwave photonic notch filter with a complex coefficient based on FWM. The complex coefficient is generated using an FD-OP. By simply controlling the phase shifts to the carrier and upper sideband, the amplitudes of the carrier and the upper sideband, this filter response is switched from bandpass filter to notch filter. The results show that the center frequency of the notch filter can be continuously tuned from 5.853 GHz to 29.311 GHz with *FSR* of 11.729 GHz and a full *FSR* is covered without changing the shape of the frequency response.

References

[1] J. Capmany, B. Ortega and D. Pastor, Journal of Lightwave Technology **24**, 201 (2006).

[2] J. Yao, Journal of Lightwave Technology **27**, 314 (2009).

[3] Capmany J., Mora J., Gasulla I., Sanchi J., Lloret J. and Sales S., Journal of Lightwave Technology **31**, 571 (2013).

[4] Minasian R. A., Chan E. H. W. and Yi X., Optics Express **21**, 22918 (2013).

[5] Zou D., Zheng X., Li S., Zhang H. and Zhou B., Optics Communications **326**, 150 (2014).

[6] Ai-ling Zhang, Cong Huang and Xiao-jun Wu, Optoelectronics Letters **10**, 5 (2014).

[7] Xu X., Ou H. and Wong K., IEEE Photonics Technology Letters **26**, 893 (2014).

[8] Feng X., Lu C., Tam H. Y. and Wai P. K. A., IEEE Photonics Technology Letters **19**, 1334 (2007).

[9] Xue X., Zheng X., Zhang H. and Zhou B., Optics Express **20**, 26929 (2012).

[10] W. Li, N. H. Zhou and L. X. Huang, IEEE Photonics Journal **3**, 462 (2011).

[11] M. Sagues, R. Garcia Olcina, A. Loayssa, S. Sales and J. Capmany, Optics Express **16**, 295 (2008).

[12] W. Li, L. X. Wang and N. H. Zhu, IEEE Photonics Journal **5**, 5501411 (2013).

[13] W. Zhang and R. A. Minasian, IEEE Photonics Technology Letters **24**, 1182 (2012).

[14] C. Zhang, L.-S. Yan, W. Pan, B. Luo, X.-H. Zou, H.-Y. Jiang and B. Lu, IEEE Photonics Journal **5**, 5501606 (2013).

[15] E. Xu and J. Yao, IEEE Photonics Technology Letters **27**, 2063 (2015).

[16] Y. Wang, E. H. W. Chan, X. Wang, X. Feng and B. Guan, IEEE Photonics Journal **7**, 5500311 (2015).